Soft Matter

Accepted Manuscript

ROYAL SOCIETY OF CHEMISTRY

www.rsc.org/softmatter

Table of Contents Graphic

Bridging and Caging in Mixed Suspensions of Microsphere and Adsorptive Microgel

Chuanzhuang Zhao, Guangcui Yuan, and Charles C. Han

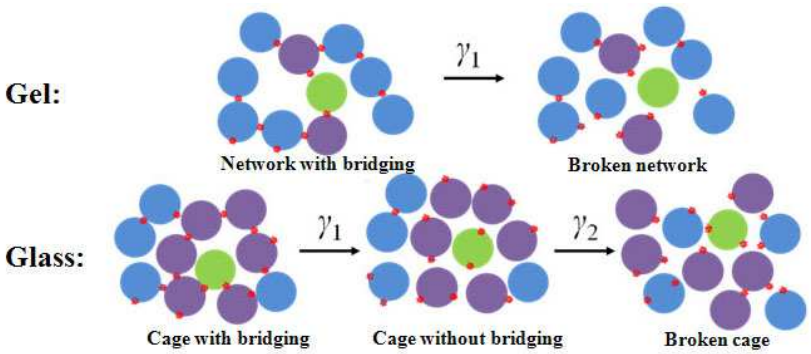

Bridging and Caging in Mixed Suspensions of Microsphere and Adsorptive Microgel

Chuanzhuang Zhao,[a,b] *Guangcui Yuan,**[,a] *and Charles C. Han**[,a]

[a] State Key Laboratory of Polymer Physics and Chemistry, Joint Laboratory of Polymer Science and Materials, Beijing National Laboratory for Molecular Sciences, Institute of Chemistry, Chinese Academy of Science, Beijing 100190, China;

[b] Department of Polymer Science and Engineering, Faculty of Materials Science and Chemical Engineering, Ningbo University, Ningbo 315211, China

Corresponding authors: Guangcui Yuan (E-mail: gcyuan@iccas.ac.cn) and Charles C. Han (E-mail: c.c.han@iccas.ac.cn)

Telephone: +86 10 82618089. Fax: +86 62521519

Abstract

Gelation and glass transition in a mixed suspension of polystyrene (PS) microsphere and poly(N-isopropylacrylamide) (PNIPAM) microgel were studied as a function of total colloid volume fraction and mixing ratio of these two components. The PNIPAM microgel, which is adsorbable to the PS microsphere surface, can induce bridging or stabilizing effect between microspheres depending on whether the volume fraction of microgel (Φ_{MG}) is smaller or larger than the saturated adsorption concentration (Φ^*_{MG}) for given volume fraction of microsphere (Φ_{MS}). Φ^*_{MG} is in a linear relationship with Φ_{MS} and the value of Φ_{MG}/Φ^*_{MG} can be taken as an approximate measure of surface coverage. A state diagram of gelation and glass transition is constructed with the short-ranged attractive interaction coming from the well-defined bridging bonding. Keeping Φ_{MG}/Φ^*_{MG} = 0.20 and increasing Φ_{MS} from 0.25 to 0.55, the mixed suspension transforms from a bridging gel into an attractive glass. Keeping Φ_{MS} = 0.45 and increasing Φ_{MG}/Φ^*_{MG} from 0.20 to 1.2, the mixed suspension changes from a bridging gel into an attractive glass and then a repulsive glass. The bridging effect and cage effect can be discriminated by the yielding behaviors in rheological measurements. In the nonlinear dynamic rheological experiments, one-step yielding corresponding to the disconnecting of bridge network is observed in bridging gel and one-step yielding corresponding to the breaking of cage is observed in repulsive glass. However, a two-step yielding behavior is found in the bridging-induced attractive glass, which is contributed from bridging effect of microgels and caging effect of the dense environment.

Introduction

The origins of non-equilibrium solid states (gel and glass) of colloidal suspension are important to both fundamental research and applied research.[1, 2] For some time, there has existed the idea that dense colloidal systems can be interpreted in the glass paradigm.[3] The state of a colloidal suspension is determined by the interactions between the colloidal particles and also the volume fraction (Φ) of the colloidal particles. "Cage" and "bond" are terms describing the origins of ergodic to non-ergodic transition in the glass paradigm for colloidal systems. Caging effect is created by increasing particle volume fraction. For hard sphere colloids, the suspension will go into a repulsive glass state when Φ reaches 0.58 or above, in which the particles are trapped 'topologically' by their neighboring particles.[4] Bonding effect refers to attractive interaction between particles. For colloidal particles with short-ranged attractive potential, the colloidal particles can bond with each other and form a continuous network at low volume fraction of colloids ($\Phi \approx 0.01$), which is called colloidal gel.[5, 6] When Φ is higher than 0.4, an attractive glass states has been predicted theoretically[7] and identified experimentally,[8] in which the particles are arrested by the interparticle bonds. For colloidal particles with long-ranged attraction, full phase separation will occur and the colloidal suspension becomes a mixture of colloid-rich phase and colloid-poor phase.

Regarding to the origins of the ergodic to non-ergodic transition, repulsive hard sphere particles stop translational motion at volume fractions about 0.58 (to form a repulsive glass) simply because they run out of space, while attractive particles lose

ergodicity (to form an attractive glass) because they stick to their neighbors. Within this framework, it is possible to treat the particle gelation phenomenon in terms of the glass theory,[11] and it seems that for some concentration regimes the details of the density correlation as gelation is approached can be well described by glass-transition ideas and laws.[3] Still, many efforts have been made trying to distinguish the difference between colloidal gel and attractive glass,[12,] and the difference between attractive glass and repulsive glass,[14] regarding to their static structure and dynamic properties. From the dynamic perspective, it has been reported that both repulsive glass and colloidal gel showed one-step yielding behavior, and attractive glass exhibited two-step yielding behavior. The one-step yielding in repulsive glass is corresponding to the breaking of the "cage",[15] and the two-step yielding of attractive glass is respectively related to the breaking of the "cage" and the breaking of the "bond".[16, 17]

The gelation and glassification in colloidal systems has been found (theoretically and experimentally) to be independent of the detailed nature of the interaction potential, and the primary control parameter is the range of the attraction (or the ratio of the attractive range to the repulsive range).[18-20] The inter-particle interaction not only can arise from the polarizability of particles or from the chemistry of particle surface, but also can arise from the addition of a third component (beside colloid and solvent) which acts as depletant agent or bridging agent. Adding a third component is an effective way to introduce attractive interaction between colloidal particles and thus to induce gelation or glass transition.[21, 22] If the added polymer is nonadsorptive

to the colloid surface, the osmotic pressure between the depletion layer and the bulk solution will drive the colloid particles to form aggregates.[23] Colloidal gels and attractive glasses can form in the presence of depletion attraction.[6, 8] If the added polymer is adsorptive to the colloid surface, the colloid particles can be stabilized by the adsorbed polymer when the concentration of the adsorptive polymer is high enough to make the surface of the colloids fully covered.[24] When the concentration of adsorptive polymer is further increased above the adsorption saturation, the extra free polymers in the solution can also cause depletion attraction. For example, in a mixed suspension of Laponite and poly(ethylene oxide), formation of an attractive glass was driven by extra free polymer chains.[25] On the other hand, if the concentration of the adsorptive polymer is too low to cover the entire colloid surface, different segments of the same polymer can be anchored to different colloid particles and aggregates will form through bridging of the polymer.[26] Under this situation, colloidal gel can also form at low Φ value.[27, 28] Although bridging is a direct way to stick colloids which leads to gel formation, the systems with bridging attraction are rarely taken as model colloidal systems in the investigation of gelation and glassification behaviors of colloids with short-range attraction.

In this paper, we reported the gelation and glassification in a mixed suspension of polystyrene (PS) microsphere and poly(N-isopropylacrylamide) (PNIPAM) microgel, where the PNIPAM microgel is adsorbable to the PS microsphere surface. For a given volume fraction of microsphere (Φ_{MS}), depending on whether the volume fraction of microgel (Φ_{MG}) is smaller or larger than the saturated adsorption

concentration (Φ^*_{MG}), the microgel can induce bridging or stabilizing effect. The bridging and stabilizing mechanisms, and the related aggregation and gelation behavior in mixed suspension of PS microspheres and PNIPAM microgels have been studied in our previous studies.[29,33] The size of microgel is significantly smaller than the size of microsphere but monodispersed and tunable through temperature.[29] In this case, the PS microspheres are taken as hard spheres, and the bridging effect of microgels which closely connect the microspheres can be considered as a kind of short-ranged attractive interaction. Therefore, the well-defined bridging bond is obtained. The important parameter, here the ratio of the attractive to the repulsive interaction, is controlled by the average number of bridging bonds on each microsphere, which is a direct result of surface coverage of microgel on the surface of microsphere.

Experiments

Materials

N-isopropylacrylamide (NIPAM, 98%, Aladdin Chemistry) was purified by recrystallization in hexane. 2, 2'-azobisisobutyronitrile (AIBN, 98%, Tianjin Yuming) was purified by recrystallization in ethanol. Styrene (98%, Sinopharm Chemical) was purified via passing through a basic alumina column to remove the inhibitor before use. Sodium dodecyl sulphate (SDS, 99%, Beijing Chemical), N, N'-methylenebisacrylamide (BIS, 99%, Alfa Aesar), ethanol (95%, Beijing Chemical) Potassium persulfate (KPS, 98%, Beijing Chemical) and polyvinylpyrrolidone (PVP,

molecular weight 30000 g/mol, Xilong Chemical) were used without further purification. Water (H_2O) was obtained from a Milli-Q water purification system (Millipore, USA).

Synthesis and Characterization of PS Microspheres

The PS microspheres with diameter of 1780 nm and 1500 nm were synthesized through a one-stage dispersion polymerization. The following procedure was used: 90 mL ethanol (for PS microspheres with diameter of 1780 nm) or 120 mL ethanol (for PS microspheres with diameter of 1500 nm) and 1.54 g PVP were added into a 250 mL three-necked reaction flask equipped with a condenser and a gas inlet. After PVP was dissolved into the ethanol at room temperature, the flask was transferred into a 70 ^{o}C oil bath and the solution was deoxygenated by bubbling argon gas for 30min. Then 5.0 g styrene dissolved with 0.054 g AIBN was added into the reaction flask. The reaction was continued for 24 h with the agitating of a magnetic stirrer. The product was collected by centrifugation and washed by ethanol and water. Powder of microspheres was obtained by lyophilisation. It has been reported that the PS microsphere synthesized through such a suspension polymerization method is stabilized by a layer of covalent bonded PVP,[30] which is a non-charged and water-soluble polymer. The thickness of the PVP layer was estimated to be 18 nm by scanning electron microscopy and dynamic light scattering, which is much smaller than the diameter of the PS microspheres. Thus, the modification of PVP layer on Φ_{MS} can be considered negligible to the size of the PS microsphere.

Synthesis and Characterization of PNIPAM Microgel

The synthesis of PNIPAM microgel was following the procedure of Senff and Richtering.[31] 1.6 g NIPAM, 0.30 g BIS and 0.3 mg SDS were dissolved in 90 mL water in a reaction flask. Argon was bubbled through the reaction mixture for 30 minutes. 0.6 g KPS was dissolved in 10 mL water and added into the flask. The reaction was continued at 60 ^{o}C for 6 h with the agitating by a magnetic stirrer. The resulting dispersion was extensively dialyzed against water until its conductivity was less than 1 mS/cm. Several dilute suspensions were prepared from the stock microgel suspersion with different dilution ratio (k). The viscosities of these dilute suspensions were measured at 25^{o}C. The effective volume fraction (Φ_{eff}) of dilute suspensions is determined from the relative viscosity (η_r) via Batchelor expression[32]: $\eta_r = 1 + 2.5\Phi_{\text{eff}} + 5.9\Phi_{\text{eff}}^2$. We obtained the relationship between Φ_{eff} and dilution ratio k. It should be noted that the Batchelor expression for volume fraction determination works only in dilute regime, because it is based on the assumption that the swelled microgel particles can be modeled as hard spheres in dilute dispersion. In current study, the volume fraction of microgel adopted is no more than 0.25, and $\Phi_{\text{MG}} = \Phi_{\text{eff}}$ is assumed. The hydrodynamic radius of microgel in dilute dispersion determined by dynamic light scattering (ALV/DLS/SLS-5022F) is 130 nm at 25 ^{o}C.

Preparation of Mixed Suspension

Dry PS microsphere powder weighed W_{MS} was dispersed in water in a 5.0 mL measuring flask. To suppress the crystallization in the microsphere suspension, PS microspheres with diameter of 1500 nm and 1780 nm were mixed at a number ratio of $N_{1500}/N_{1780} = 2.4$. The mixed microsphere suspension was homogenized by ultrasonic

wave for 30 minutes. A certain volume (V_{MG}) of PNIPAM microgel stock suspension was added to the microsphere suspension, and water was added drop by drop until the fluid level reach the tick mark (V_{Tol} = 5.0 mL). Then the mixed suspension was homogenized by ultrasonic wave at 25°C for another 30 minutes. The Φ_{MG} was known from dilution ratio k with $k = V_{MG}/V_{Tol}$ and the Φ_{MS} was calculated by $\Phi_{MS} = (W_{MS}/\rho)/V_{Tol,}$ where ρ is the density of polystyrene (1.05g/cm^3).

Instrumentation

Phase contrast microscopy was performed on a Nikon E600POL. A drop of suspension was withdrawn and placed between a microscope slide and a cover slip. Images were taken within 5 minutes after the sample was prepared, such that the evaporation of water is not significant. The viscosities of dilute microgel suspensions were measured in a Couette geometry on a stress controlled rheometer (Haake MARS). Oscillatory frequency sweeps and oscillatory strain sweeps were performed in a 50 mm cone-plate geometry and a 25 mm cone-plate geometry on a stress-controlled rheometer (Anton Paar MCR 501). As a standard protocol a high strain dynamic shear rejuvenation (γ = 1000%, ω = 1 rad/ s) was performed followed by a waiting time of typically 100 s before each experiment. Silica oil was coated on the edge of the cone-plate to prevent the water evaporation. Temperature was kept at 25 °C during the rheological measurement.

Results and Discussion

Construction of State Diagram

It has been found in our previous works that the PNIPAM microgel is adsorbable to

the PS microsphere surface and can induce bridging or stabilizing effect between microspheres depending on the mixing ratio of these two components.[29,33] A factor Φ_{MG}/Φ^*_{MG} is approximately used to evaluate the surface coverage or the extent of bridging. In very dilute colloid suspensions, the Φ^*_{MG} is determined by dynamic light scattering as the correlation function returned back to a narrow distributing single relaxation with increasing Φ_{MG}. In dilute colloid suspensions, Φ^*_{MG} is determined by optical microscopy observation as the minimum concentration of microgel needed to induce the disappearance of clusters of microsphere. In concentrated colloid suspensions, the Φ^*_{MG} is determined by rheological measurement as gel-liquid transition occurred with increasing Φ_{MG}. It is found that Φ^*_{MG} has an approximate linear relationship with Φ_{MS}. This adsorption relationship, $\Phi^*_{MG} = 0.43\times\Phi_{MS}$, is utilized in this study as indicated by the dash line in the schematic state diagram of the mixed suspension (Figure 1). This adsorption line makes a distinction between bridging and stabilizing effect. Below the dash line, $\Phi_{MG} < \Phi^*_{MG}$, the bridging effect dominates the interaction between the microspheres and the system is in a gel state. Above the dash line, $\Phi_{MG} > \Phi^*_{MG}$, the microspheres are stabilized by the adsorbed microgel, and the system is in a liquid state.

The dotted line in Figure 1 is a reference line for glass transition, along which the total volume fraction ($\Phi_{Tol} = \Phi_{MG} + \Phi_{MS}$) equals 0.58 (which is the jamming transition point of hard sphere suspension[4]). It should be noted that, the volume fraction for the occurring of glass transition should be system dependent, and the actual volume fraction of soft deformable microgel in dense environment for this

specific system is unknown. Therefore, the dotted line is a hypothetical reference line. On the right side of the dotted line, $\Phi_{Tol} > 0.58$, the caging effect becomes dominating due to the loss of free volume. Around the intersection point of the dotted line and dashed line, both the bridging and caging effects play important roles. By using these two lines, a hypothetical state diagram is constructed as a function of total colloid volume fraction and mixing ratio of these two components (Figure 1).

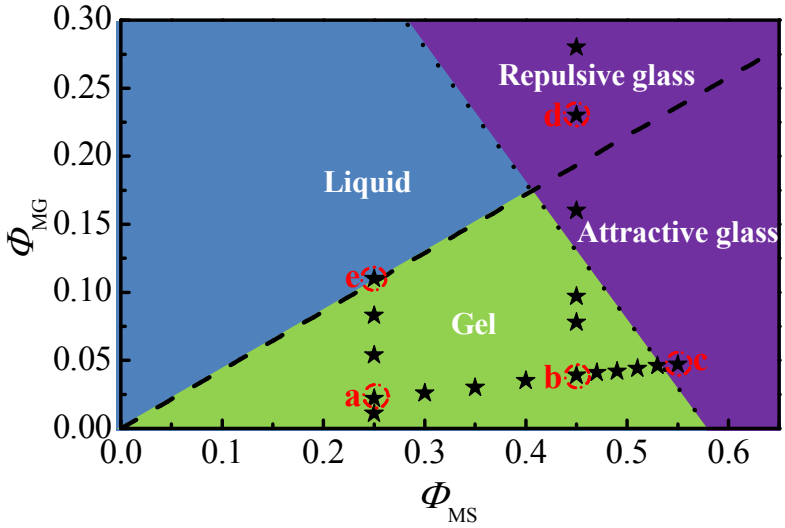

Figure 1. A hypothetical state diagram of PS microsphere and PNIPAM microgel mixed suspension. The dashed line is the adsorption line showing the minimum Φ_{MG} to stabilize the microspheres. The dotted line is the line that $\Phi_{MG} + \Phi_{MS} = 0.58$. The stars show the Φ_{MG} and Φ_{MS} of the samples that we measured in this paper. Four data points in the red circles, **a**, **b**, **c** and **d,** correspond to the Φ_{MG} and Φ_{MS} of samples measured in Figure 2 and Figure 3.

The morphology of samples in different representative regions (denoted as **a**, **b**, **c** and **d** in Figure 1) of the state diagram is shown in Figure 2. Since the mixed suspensions are turbid in bulk, a small drop of the specimen was sandwiched between two glass slides and gently pressed until a thin translucent layer was obtained. Due to

the confinement of the slides and the shearing history, the photographs showed in Figure 2 may be slightly different from the structure of the mixed suspension in bulk, but they can still inform the state transitions of the mixed suspension. In Figure 2a, 2b and 2c, the Φ_{MS} is increased from 0.25 to 0.55, while the Φ_{MG}/Φ^*_{MG} is kept almost constant at 0.20, so the bridging effect of these samples is assumed to be the same. As showed in Figure 2a, in the suspension with Φ_{MS} = 0.25, the microspheres link with each other and form a space-filling network, implying that the mixed suspension is a gel-like material. As for the suspension with Φ_{MS} = 0.45 (Figure 2b), the branches of the network are more coarsened than that in Figure 2a. At an even higher concentration (Φ_{MS} = 0.55, Figure 2c), the microspheres are crowding together and the network structure is no longer obvious, indicating that sample is probably in a jammed glassy state with bridging interaction. Figure 2d shows the morphology of a sample with Φ_{MS} = 0.45 and Φ_{MG} = 0.23 (Φ_{MG}/Φ^*_{MG} = 1.2), where the entire microsphere surface is covered by microgel and no bridges can be formed at this state. There is no sign of network structure and the distribution of microsphere is quite different from that in Figure 2b which has the same Φ_{MS}.

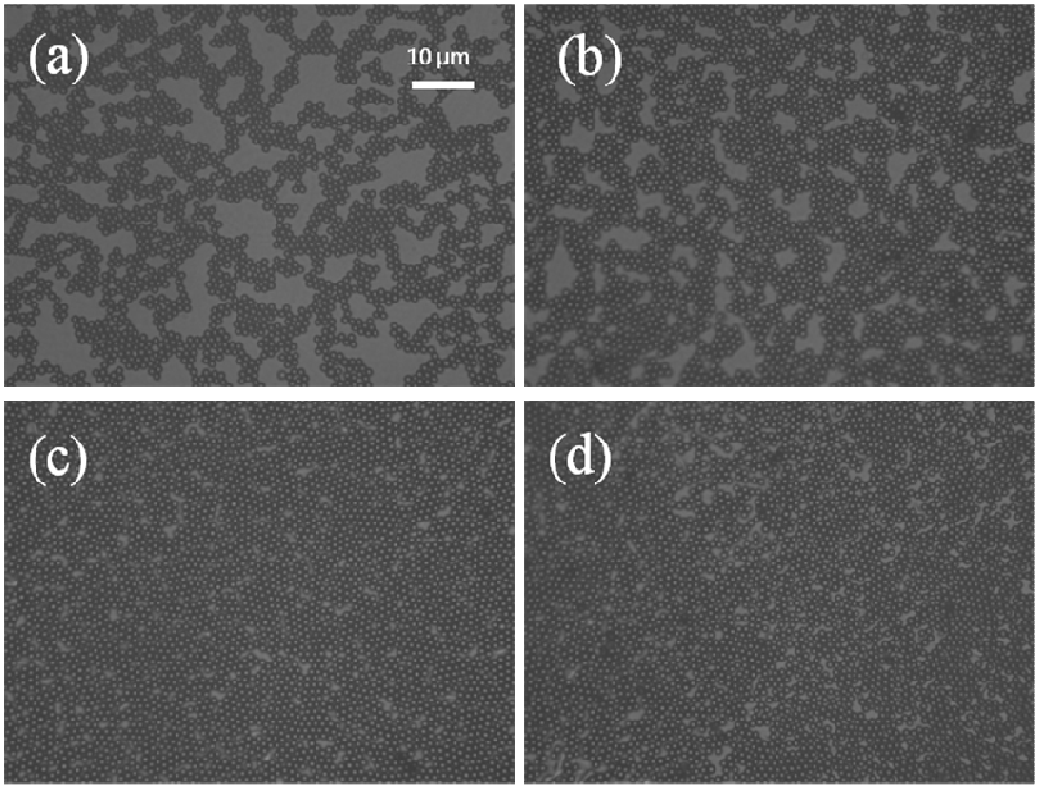

Figure 2. Optical microscopy images of the mixed suspension at different Φ_{MG} and Φ_{MS} values: (a) Φ_{MS} = 0.25, Φ_{MG} = 0.022; (b) Φ_{MS} = 0.45, Φ_{MG} = 0.039; (c) Φ_{MS} = 0.55, Φ_{MG} = 0.048; (d) Φ_{MS} = 0.45, Φ_{MG} = 0.23.

Figure 3 shows the linear angular frequency (ω) sweeps on the corresponding samples in Figure 2. All the four samples show $G' > G''$ in the measured ω range, indicating that they all have solid-like character. However, the origins of their elasticity are different. Samples **a** and **b** are gel-like materials, as the bridging network structure are clearly shown in Figure 2. The Φ_{MG}/Φ^*_{MG} of sample **c** is the same as that of sample **a** and sample **b**, so there are bridging bonds between the microspheres in sample **c**; meanwhile, the Φ_{Tol} of sample **c** is larger than 0.58, so the caging effect cannot be neglected. Therefore, for the moment, sample **c** is ascribed as the "attractive glass" state. As for sample **d**, bridging bonds cannot form since Φ_{MG} is higher than

Φ^*_{MG} that the entire surface of microspheres are covered by the mirogel. Sample **d** can be ascribed as a "repulsive glass", as its Φ_{Tot} is on the right hand side of the line of $\Phi_{Tol} = 0.58$.

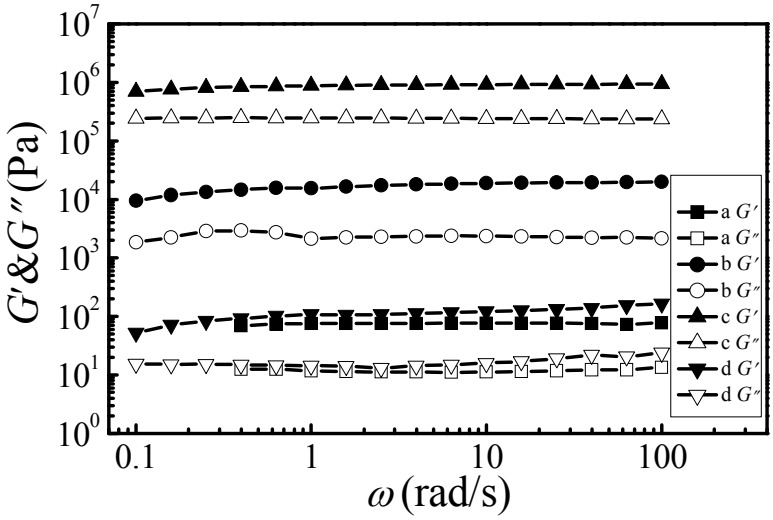

Figure 3. Angular frequency sweeps of the mixed suspension at different Φ_{MG} and Φ_{MS} values: (a) $\Phi_{MS} = 0.25$, $\Phi_{MG} = 0.022$; (b) $\Phi_{MS} = 0.45$, $\Phi_{MG} = 0.039$; (c) $\Phi_{MS} = 0.55$, $\Phi_{MG} = 0.048$; (d) $\Phi_{MS} = 0.45$, $\Phi_{MG} = 0.23$. The strain amplitude was fixed at 0.1%, which is in the linear viscoelasticity region for all the samples.

In the following sections of this paper, we will show the linear and nonlinear rheological study on different transitions, including the transitions from bridging gel to liquid (**a→e,** in Figure 1), from bridging gel to bridging attractive glass (**a→b→c,** in Figure 1) and from bridging gel to repulsive glass (**b→d,** in Figure 1). Our aim is to find out the influence of bridging and caging on the rheological behaviours of the mixed suspension, to differentiate the different solid states and to examine the reality of the hypothetical state diagram.

Transition from Bridging Gel to Liquid

The effect of bridging and stabilizing of microgels on microspheres at Φ_{MS} = 0.25 is shown in Figure 4. With Φ_{MG} = 0.022, the mixed suspension behaves as a thixotropic solid, which have higher storage modulus (G') than loss modulus (G'') at small strain amplitude (γ) and lower G' than G'' at large γ. The solid-like property is attributed to the network of the microspheres bridged by microgels, which can be seen in Figure 2a. With Φ_{MG} increasing till Φ_{MG} = 0.11, the mixed suspension behaves as a liquid because its G' is lower than G'' in the experimental range of γ, which is related to the fact that the adsorption saturation is achieved at such Φ_{MG} and no more bridging bonds can be formed. The plateau storage modulus and loss modulus at the linear viscoelastic region (G_p' and G_p''), is plotted as a function of Φ_{MG} in the inset of Figure 4. The G_p' is firstly lower than G_p'' then higher and then lower again, indicating a liquid – bridging gel – liquid transition. The modulus firstly increases then decreases, and the maximum modulus is obtained at half coverage. These phenomena can be explained by the La Mer's theory[34] on the bridging flocculation. To form a bridge, it requires at least one surface site of microsphere to be covered by the microgel and another surface site remaining uncovered. Then, the extent of bridging is proportional to $\theta(1-\theta)$, where θ is the surface coverage of the microsphere employing the concept of the Langmuir isotherm absorption. Therefore, the maximum of bridging extent appears at θ = 0.5. Detailed study on the gel-liquid transition of a similar system can be found in our previous work.[33]

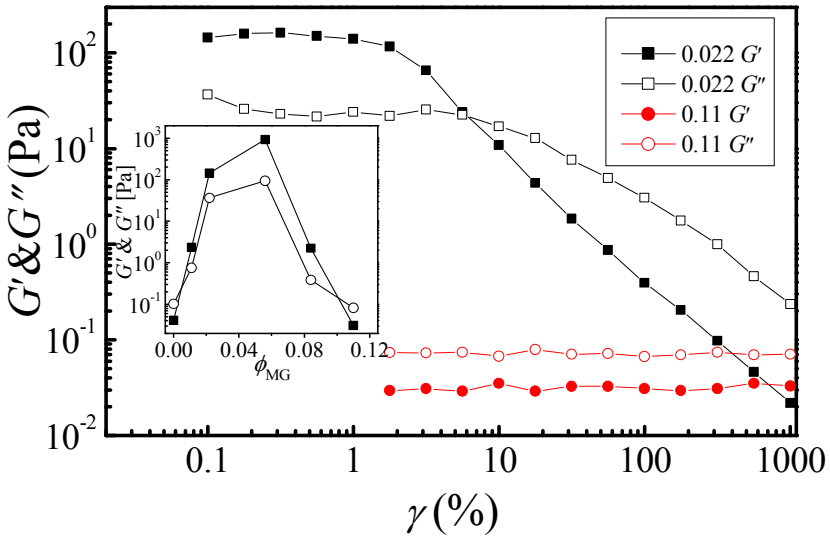

Figure 4. Oscillatory strain sweeps of mixed suspension with different Φ_{MG} but constant Φ_{MS} 0.25. The angular frequency (ω) of the sweeps was 1 rad/s. The Φ_{MG} was shown in the box. The inset figure shows the dependence of plateau modulus against Φ_{MG}.

Transition from Bridging Gel to Bridging Attractive Glass

To understand the influence of caging effect on the bridging microsphere suspension, oscillatory strain sweeps (angular frequency ω = 1 rad/s) were performed on mixed suspensions with different Φ_{MS} and fixed Φ_{MG}/Φ^*_{MG} = 0.2 (along **a** → **c** line in Figure 1). All the samples exhibit linear viscoelasticity at small strain, and the G_p' is plotted against Φ_{MS}. As shown in Figure 5, there is a turning point at about Φ_{MS} = 0.47. As $\Phi_{Tol} < 0.47$, the data can be fitted by a power-law scaling (red dash line in Figure 5). Such a power law increasing of G' against Φ_{MS} is usually found in colloidal gel with polymer-bridging[35] or short-ranged attraction[36]. As $\Phi_{MS} \geq 0.47$, the storage modulus increases dramatically and deviates from the power-law scaling line. This phenomenon resembles the behavior of hard sphere glasses approaching the glass

transition,[37] indicating that the effect of caging begins to play a role.

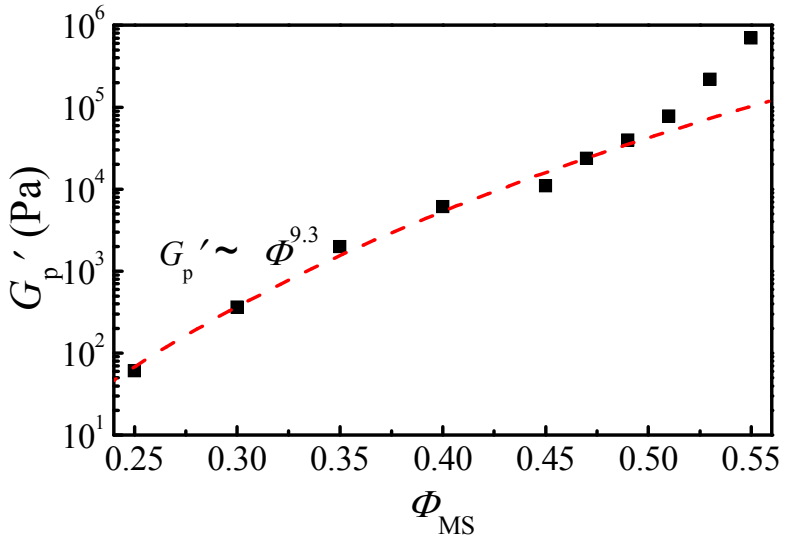

Figure 5. Plateau storage modulus at linear viscoelastisity region (G_p') as a function of Φ_{MS} with $\Phi_{MG}/\Phi^*_{MG} = 0.20$. The red dash line is the fitting of the data using $G_p' \sim \Phi_{MS}^{9.3}$.

The results of oscillatory strain sweeps of the mixed suspensions with different Φ_{MS} but constant $\Phi_{MG}/\Phi^*_{MG} = 0.2$ are shown in Figure 6a. At small strain amplitude γ ($\gamma <$ 3% and $\omega = 1$ rad/s), the values of G' and G'' of all the samples stay constant and $G' > G''$, indicating the solid-like character. With γ reaches 3%, the values of G' and G'' start to drop and the decreasing of G' is much faster than G'', and finally $G' < G''$, which indicates that the samples become a liquid-like material under large amplitude of deformation. The power-law dependence at high strain (straight line in the log-log plots) is a typical fluid-like response. For sample with $\Phi_{MS} = 0.55$, the transition from solid-like to liquid-like character is not observed immediately after the crossover between G' and G''. Over a broad range of strains, the decay of the two moduli is weaker, indicating that some residual structure remains under flow. Interestingly,

there are another inflexion points on both the curves of G' and G'' at about γ = 30%, implying a two-step yielding behavior.

The features of two-step yielding determined from $G'(\gamma)$ and $G''(\gamma)$ plots are not very conspicuous. To present the yielding behaviors more clearly, the stress amplitude (σ) is plotted against strain amplitude γ in Figure 6b, as an alternative representation of the same data in Figure 6a. The maxima or shoulders on plots in Figure 6b support the presence of two yielding process. The locating of yielding points can be quantitatively identified by the maxima in Figure 6b and are plotted against the Φ_{MS} in Figure 6c. As shown in Figure 6b, at small γ (γ < 3%), σ increases linearly with γ, implying that the material responses to the applied deformation elastically. After this yielding peak, the curves of the samples with Φ_{MS} < 0.47 become a plateau, indicating a completely yielding;[15] while the curves of the samples with $\Phi_{MS} \geq$ 0.47 exhibits another peak, indicating a two-step yielding behavior. As shown in Figure 6c, the first yielding strain (γ_1) keeps almost constant at different Φ_{MS}. On the other hand, with decreasing Φ_{MS}, the second yielding peak becomes less and less prominent (Figure 6b) meanwhile its position shifted to larger γ (Figure 6c).

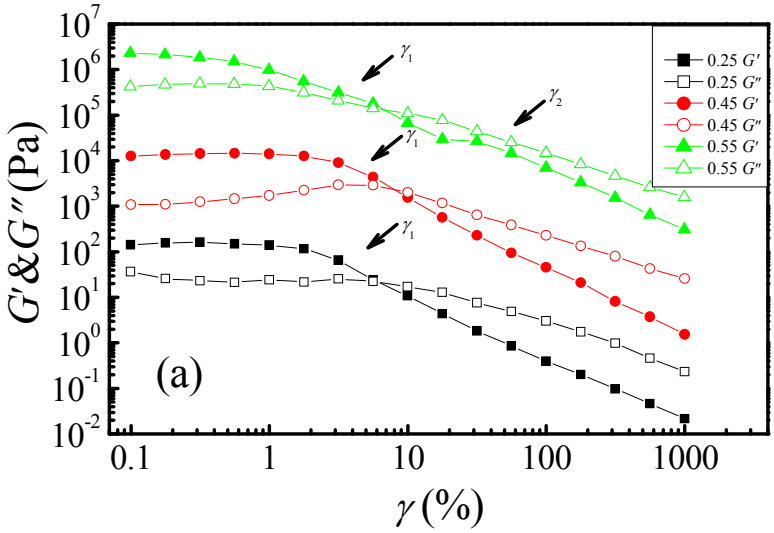

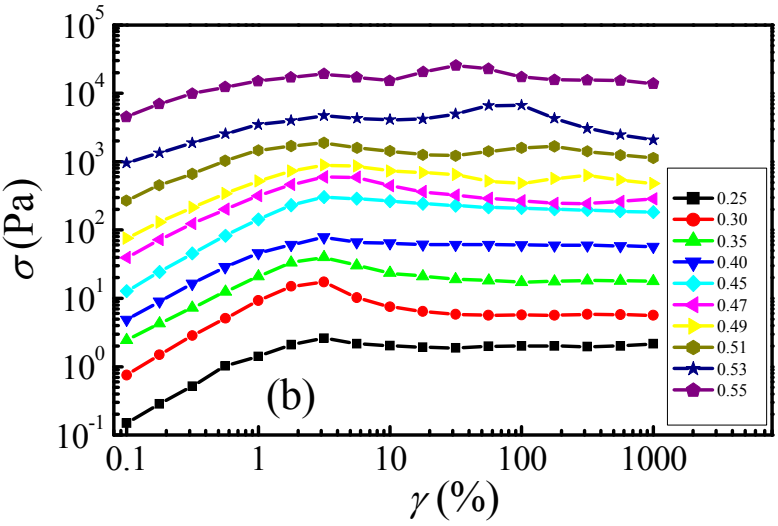

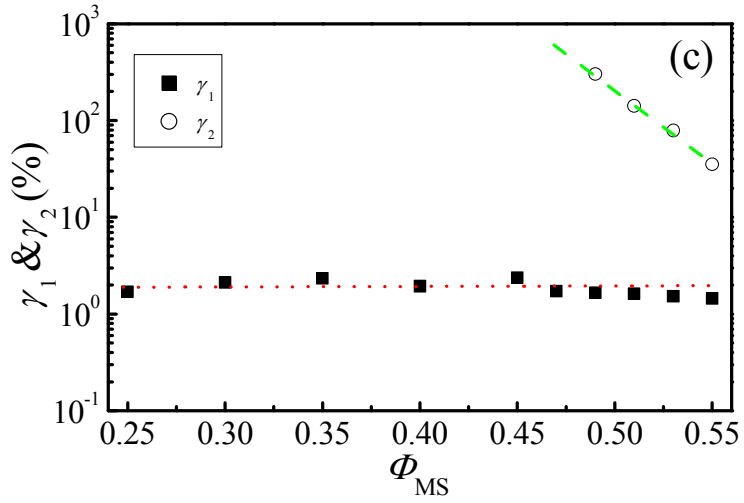

Figure 6. Oscillatory strain sweeps of mixed suspension with different Φ_{MS} and constant $\Phi_{MG}/\Phi^*_{MG} = 0.20$: (a) G' and G'' as a function of γ; (b) σ as a function of γ; (c) γ_1 and γ_2 as a function of Φ_{MG}. The Φ_{MS} is denoted in the inset box of the plots in (a) and (b). The angular frequency (ω) of the sweeps was 1 rad/s. The arrows in (a) indicates the location of yielding points. The red dot line and the green dash line in (c) are guides for the eyes.

A schematic model is proposed in Figure 7 to explain the yielding behavior of the mixed suspension. For mixed suspension with low concentration of microsphere (Φ_{MS} < 0.47), there is a network structure with bridging bonds (Figure 7a). When a small strain ($\gamma < \gamma_1$) is applied on the suspension, the microspheres will vibrate by stretching or compressing their bridging bonds but will not destroy the network. However, with the strain increasing, the oscillatory motion will intensify the stimulation on displacement of each microsphere, and bridging bonds will start to break up. When $\gamma > \gamma_1$, the network can be broken and the whole system gains its fluidity. In this case, the yielding strain may be determined by the average number of bridging bonds on each microsphere which is directly related to the surface coverage. As Φ_{MG}/Φ^*_{MG} is

fixed at 0.20, so the surface coverage of each sample can be assumed to be the same, and the values of the first yielding strain γ_1 remain unchanged with Φ_{MS} (Figure 6c).

For denser mixtures ($\Phi_{MS} \geq 0.47$), the bridging bonds between microspheres are similar to the low Φ_{MS} samples, but the dynamic arresting effect of caging also begin to play a role due to crowded environment (Figure 7b). The bridging bonds of the denser suspension break at $\gamma = \gamma_1$. However, before γ reaches γ_2, the disconnected microspheres are still confined and rattling in the cages constructed by their surrounding microspheres, and can only explore the free volume inside the cage. This will last until γ reaches γ_2, when the deformation of the system is large enough to break the cages and release each microsphere. The denser the system is, the less free volume will be left for the microspheres to adjust their positions and to catch up with the deformation of the whole system, and hence the smaller deformation the cages could bear. Therefore, γ_2 decreases as the increasing of Φ_{MS}, as indicated in Figure 6c.

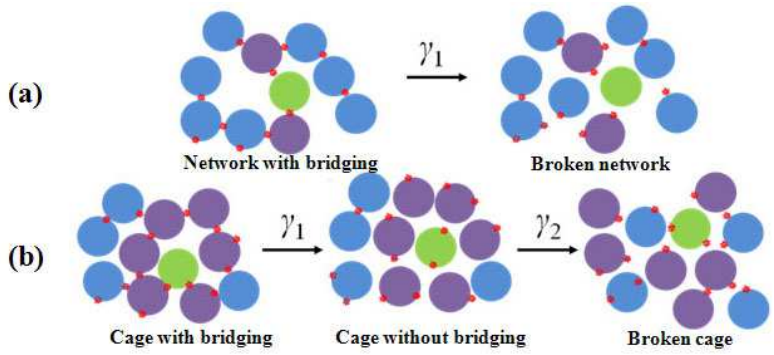

Figure 7. A schematic illustration of the yielding mechanism of bridging gel (a) and bridging attractive glass (b). The purple spheres are the neighboring microspheres bonding with or caging the target microsphere (green sphere). The blue spheres are other microspheres which are not belong to the cage, and the small red spheres are microgels.

Transition from Bridging Gel to Repulsive Glass

The oscillatory strain sweeps experiments were also performed on samples with different values of Φ_{MG}/Φ^*_{MG} but constant $\Phi_{MS} = 0.45$ (along **b** → **d** in Figure 1). As shown in Figure 8, all samples show $G' > G''$ at small strain and $G' < G''$ at large strain, which indicates that the samples have solid-like character at small strain and fluid-like character at large strain. With Φ_{MG} increasing, the modulus of the mixed suspension firstly increases (Figure 8a), then decreases (Figure 8b). For the samples with $\Phi_{MG} = 0.039$ and $\Phi_{MG} = 0.078$, one-step yielding behaviour is observed, which is corresponding to the breaking of bridging bonds. For the samples with $\Phi_{MG} = 0.097$ and $\Phi_{MG} = 0.16$, besides the first yielding of bond breaking, another inflexion point can be recognized at larger strain, which is attributed to the breaking of cages. For the samples with $\Phi_{MG} = 0.23$ or $\Phi_{MG} = 0.30$, only one-step yielding behaviour is presented again, which is ascribed as the breaking of the cages. The yielding strains of bond breaking (γ_1) and cage breaking (γ_2) are plotted against Φ_{MG} (Figure 8c). It is found that γ_1 firstly decreases with Φ_{MG} then increases, while γ_2 decreases with Φ_{MG} in the whole experimental range.

For a constant Φ_{MS}, two effects can be introduced by gradually increasing Φ_{MG}. On one hand, the surface coverage of each microsphere will be increased to 0.5 then to 1, so the density of bridging bonds will first increase and then decrease. On the other hand, with increasing the Φ_{MG}, the total volume fraction of the microgel and microsphere will increase, where the caging effect becomes more and more significant. In Figure 8a, as Φ_{MG} increases from 0.039 to 0.097, the corresponding

Φ_{MG}/Φ^*_{MG} increases from 0.20 to 0.50, therefore the average number of bridging bonds increase. The branches of the microsphere network become more rigid, so the microsphere network can bear larger stress but smaller deformation. These are demonstrated from the phenomenon that the plateau values of G' and G'' increase and the yielding strain shifted to lower value. As Φ_{MG} increases from 0.097 to 0.23, the corresponding Φ_{MG}/Φ^*_{MG} increases from 0.5 to 1.2, more surface areas are occupied by the microgel so density of bridging bonds decreases. Less bridging bonds will make the microsphere network weaker and more flexible, and this can be told from smaller modulus and larger yielding strain. Meanwhile, due to the more and more crowding environment, the second yield strain, which corresponds to the breaking of the cages, begins to show up. As $\Phi_{MG} = 0.23$ and $\Phi_{MG} = 0.28$, the entire surface of the microsphere is covered by the microgel and the total volume fraction of the systems is very high, therefore, these two samples shall be ascribed to a repulsive glass, and its single yielding shall be corresponded to the breaking of cage. The decreasing of γ_2 with the increasing of Φ_{MG} in Figure 8c can be explained as the loss of free volume and the densification of the cage.

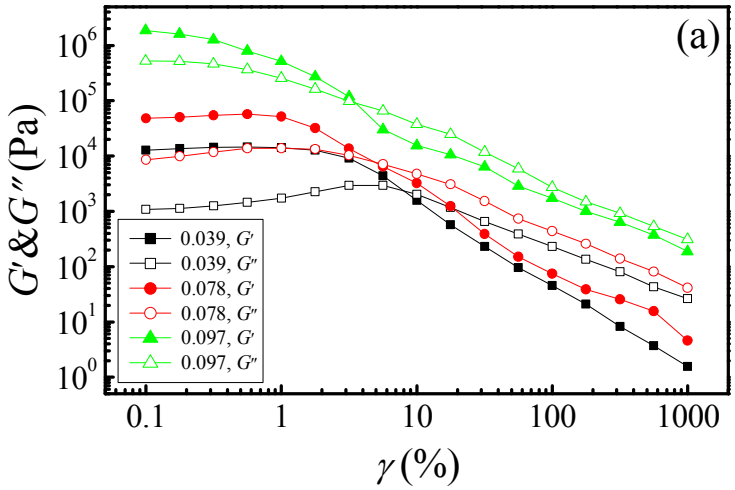

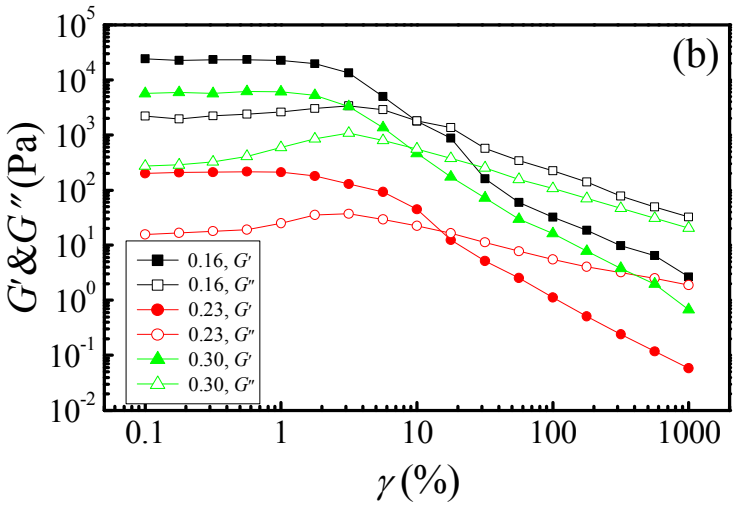

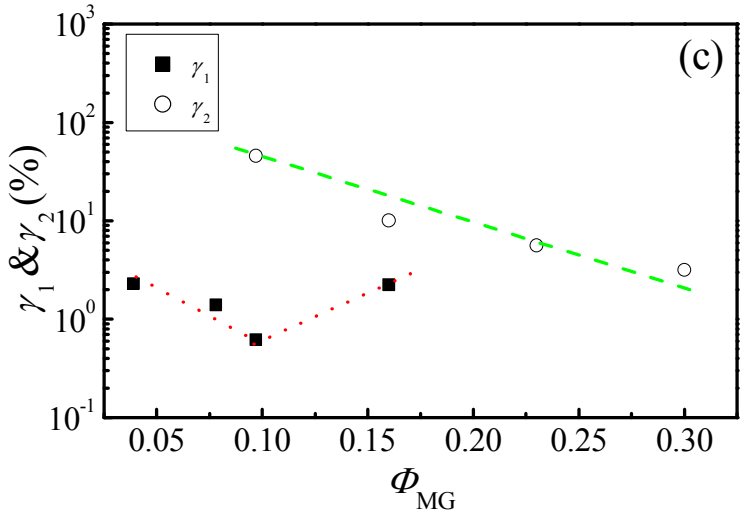

Figure 8. Oscillatory strain sweeps of mixed suspensions at different Φ_{MG} and Φ_{MS} was fixed at 0.45. (a) $\Phi_{MG}/\Phi^*_{MG} \leq 0.5$; (b) $\Phi_{MG}/\Phi^*_{MG} \geq 0.5$; (c) γ_1 and γ_2 as a function of Φ_{MG}. The Φ_{MG} was denoted in the inset box of the plots in (a) and (b). The angular frequency (ω) of the sweeps was 1 rad/s. The red dotted line and the green dashed line are guides for the eyes.

The interplay of bridging and caging studied in current work can be associated with the study of arresting mechanisms and dynamical heterogeneity in colloidal gel and colloidal glasses. It has been reported that the arresting and dynamical heterogeneity arises from the bonding of the particles (cluster formation) for the gels and attractive glasses, while from the crowding of the particles (caging) for the hard sphere glasses.[14,38] However, as for crowded attractive colloid suspension, a detailed understanding of the competition between the two arresting mechanisms has not been achieved. Simulation works of Chaudhuri et al.[39] show a multi-step decay of time –correlation functions of an attractive colloidal system, which indicates the coexistence of two distinct length scales and well-separated time scales for cage/bond relaxation. The experimental result of two-step yielding in the present work may be a

consequence of the two different arresting mechanisms. Zaccarellia and Poon[40] suggested that the arrest in an attractive glass is, in the long run, topological. As Figure 6c and Figure 8c shows, γ_2 tend to merge with γ_1, if concentrating the system by increasing Φ_{MS} and Φ_{MG} or decreasing the bond numbers by tune the Φ_{MG}/Φ^*_{MG}. This tendency implies that the difference between the two arresting and dynamical heterogeneity mechanisms become smaller in their time scale and length scale as the increasing the concentration or decreasing the attraction.

Conclusions

The bridging and caging effect induced by adsorptive PNIPAM microgel on the PS microspheres was studied in this work. When the concentration of the microgel is lower than the saturated adsorption concentration for a given volume fraction of microsphere, there exist the microgel bridges which link the microspheres together. Increasing the volume fraction of the microsphere (Φ_{MS} = 0.25 ~ 0.55) at a constant surface coverage (Φ_{MG}/Φ^*_{MG} = 0.20), the mixed suspension transforms from a bridging gel to an attractive glass, which is due to the caging effect at high volume fraction. Increasing the volume fraction of the microgel (Φ_{MG}/Φ^*_{MG} = 0.20 ~ 1.2) while keeping the volume fraction of the microsphere at constant (Φ_{MS} = 0.45), the system changes from a bridging gel into an attractive glass and then a repulsive glass, which is due to the interplay between bridging and caging. In the nonlinear dynamic rheological experiments, the bridging gel shows a one-step yielding corresponding to the disconnecting of the bridged network, the repulsive glass also shows a one-step yielding corresponding to the breaking of the cage, while attractive glass shows a

two-step yielding corresponding to the disconnecting of the bridged network and the breaking of the cage. It should be noted that the two-step yielding behavior is not a unique feature of the attractive glass with bridging bonds. Colloidal glasses with depletion attractions[14-16] with van der Waals attractions,[41] or with magnetic interaction force[42] are also found to show such two-step yielding behavior, suggesting that such behavior may be independent of the physical nature of the attraction. The results exhibited in this paper can shed new lights on the understanding of the relationship between bonding and caging in the attractive colloidal glasses. Also, these results are believed to be helpful in formulating soft materials, especially in tuning the properties of colloidal suspensions by adding polymers.

Acknowledgement

This work is supported by the National Basic Research Program of China (973 Program, 2012CB821503).

References

1 J. Mewis and N. J. Wagner, *Colloidal Suspension Rheology*, Cambridge University Press, Cambridge; New York, 2012.
2 W. C. K. Poon, *Science*, 2004, **304**, 830-831.
3 K. A. Dawson, *Curr. Opin. Colloid Interface Sci.*, 2002, **7**, 218-227.
4 E.R. Weeks and D.A. Weitz, *Phys. Rev. Lett.*, 2002, **89**, 095704.
5 P. J. Lu, E. Zaccarelli, F. Ciulla, A. B. Schofield, F. Sciortino and D. A. Weitz, *Nature*, 2008, **453**, 499-503.
6 E. Zaccarelli, *J. Phys.: Condens. Matter*, 2007, **19**, 323101.
7 K. Dawson, G. Foffi, M. Fuchs, W. Götze, F. Sciortino, M. Sperl, P. Tartaglia, T. Voigtmann and E. Zaccarelli, *Phys. Rev. E: Stat., Nonlinear, Soft Matter Phys.*, 2000, **63**, 011401.
8 K. N. Pham, A. M. Puertas, J. Bergenholtz, S. U. Egelhaaf, A. Moussaid, P. N. Pusey, A. B. Schofield, M. E. Cates, M. Fuchs and W. C. K. Poon, *Science*, 2002, **296**, 104-106.
9 L. J. Teece, M. A. Faers and P. Bartlett, *Soft Matter*, 2011, **7**, 1341-1351.
10 V. Trappe, V. Prasad, L. Cipelletti, P. Segre and D. Weitz, *Nature*, 2001, **411**, 772-775.
11 H. Verduin, J. K. G. Dhont, *J. Colloid Interface Sci.*, 1995, **172**, 425-437.
12 H. Tanaka, J. Meunier and D. Bonn, *Phys. Rev. E: Stat., Nonlinear, Soft Matter Phys.*, 2004, **69**, 031404.
13 A.D. Dinsmore and D. A. Weitz, *J. Phys.: Condens. Matter*, 2002, **14**, 7581.

14 Z. Zhang, P. J. Yunker, P. Habdas, and A. G. Yodh, *Phys. Rev. Lett.*, 1995, **107**, 208303
15 K. N. Pham, G. Petekidis, D. Vlassopoulos, S. U. Egelhaaf, W. C. K. Poon and P. N. Pusey, *J. Rheol.*, 2008, **52**, 649-676.
16 K. N. Pham, G. Petekidis, D. Vlassopoulos, S. U. Egelhaaf, P. N. Pusey and W. C. K. Poon, *Europhys. Lett.*, 2006, **75**, 624-630.
17 N. Koumakis and G. Petekidis, *Soft Matter*, 2011, **7**, 2456-2470.
18 G. Foffi, K. A. Dawson, S. V. Buldyrev, F. Sciortino, E. Zaccarelli, and P. Tartaglia, *Phys Rev E: Stat., Nonlinear, Soft Matter Phys.*, 2002, **65**, 050802.
19 J. Bergenholtz, M. Fuchs and T.Voigtmann, *J. Phys.: Condens. Matter*, 2000, **12**, 6575–6583.
20 K. Dawson, G. Foffi, G. D. McCullagh, F. Sciortino, P. Tartaglia and E. Zaccarelli, *J. Phys.: Condens. Matter*, 2000, **14**, 2223–2235.
21 A. Yethiraj, *Soft Matter*, 2007, **3**, 1099-1115.
22 D. Kleshchanok, R. Tuinier and P. R. Lang, *J. Phys.: Condens. Matter*, 2008, **20**. 073101.
23 S. Asakura and F. Oosawa, *J. Polym. Sci.*, 1958, **33**, 183-192.
24 E. Dickinson, *J. Chem. Soc., Faraday Trans.*, 1995, **91**, 4413-4417.
25 K. Atmuri, G. A. Peklaris, S. Kishore and S. R. Bhatia, *Soft Matter*, 2012, **8**, 8965-8971.
26 R. Evans and D. Napper, *Nature*, 1973. **246**, 34-25.
27 S. Miyazaki, T. Karino, H. Endo, K. Haraguchi and M. Shibayama, *Macromolecules*, 2006, **39**, 8112-8120.
28 K. Pickrahn, B. Rajaram and A. Mohraz, *Langmuir*, 2009, **26**, 2392-2400.
29 C. Z. Zhao, G. C. Yuan and C. C. Han, *Macromolecules*, 2012, **45**, 9468-9474.
30 J. S. Song, L. Chagal and M. A. Winnik, *Macromolecules*, 2006, **39**, 5729-5737.
31 H. Senff and W. Richtering, *Journal of Chemical Physics* **1999**, *111*, 1705.
32 G. Batchelor, *J. Fluid Mech.*, 1977, **83**, 97-117.
33 C. Z. Zhao, G. C. Yuan, D. Jia and C. C. Han, *Soft Matter*, 2012, **8**, 7036-7043.
34 V. K. La Mer, *Discuss. Faraday Soc.*, 1966, **42**, 248-254.
35 M. Surve, V. Pryamitsyn and V. Ganesan, *Phys. Rev. Lett.*, 2006, **96**, 177805.
36 J. S. Shay, S. R. Raghavan and S. A. Khan, *J. Rheol.*, 2001, **45**, 913-927.
37 T. G. Mason and D. A. Weitz, *Phys. Rev. Lett.*, 1995, **75**, 2770-2773
38 A. Coniglio, T. Abete, A. de Candia, E. Del Gado and A. Fierro, *J. Phys.: Condens. Matter*, 2008, **20**,494239.
39 P. Chaudhuri, L. Berthier, P. Hurtado and W. Kob, *Phys. Rev. E: Stat., Nonlinear, Soft Matter Phys.*, 2010, **81**, 040502.
40 E. Zaccarelli and W. C. K. Poon, *Proc. Natl. Acad. Sci. U. S. A.*, 2009, 106, 15203-15208.
41 R. C. Kramb and C. F. Zukoski, *J. Phys.: Condens. Matter*, 2011, **23**, 035102.
42 J. P. Segovia-Gutiérrez, C. L. A. Berli, and J. de Vicente, *J. Rheol*., 2012, **56**, 1429-1448.